Stimulated Glucose Uptake in the Ischemic Border Zone: Its Dependence on Glucose Uptake in the Normally Perfused Area

Yuriko Yamane, Nobumasa Ishide, Yutaka Kagaya, Daiya Takeyama, Nobuyuki Shiba, Masanobu Chida, Tetsuji Nozaki, Toshihiro Takahashi, Tatsuo Ido and Kunio Shirato

The First Department of Internal Medicine, Tohoku University School of Medicine; and Cyclotron and Radioisotope Center, Tohoku University, Sendai, Japan

During acute regional myocardial ischemia, a "border zone" exists where the spatial distributions of blood flow and substrate uptake show gradual changes. We investigated the relationship between blood flow and glucose uptake in the border zone during acute regional ischemia. **Methods:** Newly developed quantitative autoradiography using imaging plates and two long-lived radioisotopes was applied to rat hearts subjected to 30 min of left coronary artery occlusion. Blood flow, glucose uptake and fatty acid uptake was assessed with 4-[*N*-methyl-^{14}C]iodoantipyrine, 2-deoxy-D-[1-^{3}H]glucose (^{3}H-DG) and β-methyl[1-^{14}C]heptadecanoic acid (^{14}C-BMHDA), respectively. **Results:** In rats showing ^{3}H-DG uptake in the normally perfused area (Norm) of 254 ± 96 Bq/mg (high-DG) and 56 ± 20 Bq/mg (low-DG) (n = 4 for each), ^{3}H-DG uptake in the border zone was 148 ± 52 Bq/mg and 58 ± 15 Bq/mg ($p < 0.05$ high- versus low-DG), respectively. The relationship between blood flow and ^{3}H-DG uptake in the border zone was altered by the different ^{3}H-DG uptake levels in Norm. In high-DG, ^{3}H-DG uptake in the border zone was reduced significantly according to the decrease in the percentage of blood flow. However, in low-DG, no significant differences in ^{3}H-DG uptake were found among the regions in the border zone with different levels of the percentage of blood flow, except in the region with 10%–19% of the percentage of blood flow. In the border zone, the percentage of ^{3}H-DG uptake per unit blood flow normalized to that in Norm increased according to the decrease in the percentage of blood flow, and this increase was steeper in low-DG than in high-DG ($p < 0.0005$). The percentage of ^{14}C-BMHDA uptake was lower than the percentage of ^{3}H-DG uptake (27 ± 3% versus 78 ± 18% of that in Norm, $p < 0.0005$) in the peripheral ischemic area. **Conclusion:** The relationship between blood flow and glucose uptake in the ischemic border zone was altered by the different glucose uptake levels in Norm. Glucose uptake in the border zone was higher in rats with higher glucose uptake levels in Norm, suggesting that glucose uptake in the border zone stimulated by ischemia can be accelerated still more by humoral factors.

Key Words: regional myocardial ischemia; myocardial glucose metabolism; myocardial fatty acid metabolism; imaging plate; double-tracer autoradiography

J Nucl Med 1997; 38:1515–1521

Free fatty acids are the major substrates of the normally perfused myocardium in the fasting state (*1*). In the ischemic myocardium, however, glucose extraction increases concurrently with the formation of lactate, suggesting that ischemia enhances glycolysis (*1–3*). Imaging of myocardial glucose uptake by PET has been performed widely to estimate myocardial viability in patients with myocardial infarction (*4,5*).

A transient area, namely the "border zone," is reported to exist between the normally perfused area and the central ischemic area during the early phase of regional myocardial ischemia (*6–10*). Methodologies with high spatial resolution are necessary to determine the heterogeneous characteristics of myocardial cells in the border zone (*6,9,10*). However, the spatial resolution of PET is not sufficient for studying myocardial metabolism in the border zone (*11*). The tissue sampling method (*12–14*) is also unsuitable for depicting the spatial distribution of myocardial metabolism in the border zone. Recently, we developed a quantitative double-tracer autoradiography with ^{3}H and ^{14}C using imaging plates (*15*). This method can be used to determine the metabolic changes in the border zone because it has high spatial resolution (pixel area = 50 × 50 μm), high sensitivity and superior linearity over the entire dynamic range of 10^{4}–10^{5}. In this study, we applied this method to a rat model of acute regional ischemia to clarify the relationship between regional myocardial blood flow and glucose uptake in the ischemic border zone.

MATERIALS AND METHODS

The purpose and nature of this study were approved by the Committee of Animal Experiments in the Cyclotron and Radioisotope Center at the Tohoku University. Sixteen male Wistar rats, weighing 304 ± 31 g (mean ± s.d.), were fed normal rat chow and tap water ad libitum until they were subjected to the surgical procedure, which began at about 3 p.m. The rats were anesthetized with an intraperitoneal injection of sodium pentobarbital (40 mg/kg). Catheters were placed in the right common carotid artery for monitoring arterial blood pressure and arterial blood sampling and in the right jugular vein for the administration of radiopharmaceuticals. After left thoracotomy under artificial ventilation, a snare (6–0 nylon) was placed around the left coronary artery (LCA). Arterial blood was sampled for the determination of plasma concentrations of glucose (*16,17*), insulin (*18*) and free fatty acids (*19*). After the injection of 1 mg/kg lidocaine to prevent ventricular arrhythmias, the LCA was ligated.

In Group A (n = 8), 3.7 MBq 2-deoxy-D-[1-^{3}H]glucose (^{3}H-DG), with specific activity of 640 GBq/mmol (*20*), were injected intravenously for 30 sec just after the LCA ligation. Thirty minutes after the ^{3}H-DG injection, 0.185 MBq 4-[*N*-methyl-^{14}C]iodoantipyrine (^{14}C-IAP), with specific activity of 2.2 GBq/mmol (*21*), dissolved in 1.8 ml of 0.9% NaCl solution was injected intravenously at a constant rate for 30 sec with an infusion pump. Serial arterial blood samples were collected (0, 1, 3, 5, 8, 13, 18, 23 and 28 sec after the initiation of the ^{14}C-IAP infusion) to determine blood ^{14}C-IAP activities with a liquid scintillation counter. Thirty seconds after the initiation of the ^{14}C-IAP infusion, the rats were killed by cutting the ascending aorta and the pulmonary trunk. The hearts were excised rapidly and frozen in dry ice.

Received May 21, 1996; revision accepted Oct. 23, 1996.

For correspondence or reprints contact: Kunio Shirato, MD, First Department of Internal Medicine, Tohoku University School of Medicine, 1-1 Seiryo-machi, Aoba-ku, Sendai 980-77, Japan.

In Group B (n = 8), 3.7 MBq ^{3}H-DG were injected intravenously for 30 sec just after the LCA ligation, and 30 sec after that, 0.185 MBq β-methyl[1-^{14}C]heptadecanoic acid (^{14}C-BMHDA), with specific activity of 2.13 GBq/mmol (*22,23*), dissolved in 0.2 ml of an aqueous solution of bovine serum albumin (*24*) was injected intravenously for 30 sec. Thirty minutes after the ^{3}H-DG injection, the rats were injected intravenously with 2% methylene blue solution (0.5 ml) to demarcate the ischemic area by negative staining (*15*). Immediately afterwards, the rats were killed by administration of saturated KCl solution (0.3 ml). The hearts were removed rapidly and frozen in dry ice.

Quantitative Autoradiography

Quantitative double-tracer autoradiography with ^{3}H and ^{14}C was performed as described previously (*15*). In brief, 20-μm-thick frozen heart sections taken perpendicular to the long axis of the left ventricle were prepared. The sections along with the ^{3}H- and ^{14}C-labeled graded standards were placed in contact with tritium-sensitive imaging plates (TR-IP) for 2 wk and with general use imaging plates (UR-IP) for another 2 wk.

The autoradiograms were analyzed using a computer-assisted, imaging-processing system (*15*). On the color monitor display of the image processor, about 500 circular regions of interest (ROIs) (the area of each ROI was 0.0925 mm^2) were placed throughout the left ventricular wall of the midventricular level section. We put the ROIs on the TR image at the same site as the UR image using the traced film. The autoradiographic intensity of ^{14}C-IAP and ^{14}C-BMHDA was determined using the UR image. The autoradiographic intensity of ^{3}H-DG was determined by subtracting the value of the ROI of the UR image from that of the ROI of the TR image. For further analysis, we converted the autoradiographic intensity into tissue ^{3}H and ^{14}C content using the calibration lines obtained from the ^{3}H- and ^{14}C-labeled graded standards.

We determined both the myocardial blood flow (*21*) and ^{3}H-DG uptake of each ROI in Group A. Regional myocardial ^{3}H-DG uptake per unit blood flow (DG/BF), which reflects the glucose extraction (*13,14*) also was calculated in Group A. We determined both the ^{3}H-DG uptake and the ^{14}C-BMHDA uptake of each ROI in Group B. The percentages of blood flow, ^{3}H-DG uptake, DG/BF and ^{14}C-BMHDA uptake were obtained by normalizing regional values to the mean value of all ROIs in the normally perfused area in each rat.

In Group A, the normally perfused area and the ischemic area were determined as the areas showing normal and reduced concentrations of ^{14}C-IAP, respectively. In our preliminary experiments, we confirmed that the normally perfused area determined with ^{14}C-IAP agreed with that determined with methylene blue solution in rat hearts injected with both ^{14}C-IAP and methylene blue solution. We defined the ischemic border zone as the ischemic area showing more than 10% of the percentage of blood flow and the central ischemic area as the ischemic area showing less than 10%. To analyze the relationship between myocardial blood flow and ^{3}H-DG uptake, the ROIs in the border zone were classified according to their percentage of blood flow. In Group B, we defined the peripheral ischemic area as the ischemic area showing more than 10% of the percentage of ^{14}C-BMHDA uptake and the central ischemic area as the ischemic area showing less than 10%.

Noise Due to Subtraction Method

The ^{3}H intensities obtained by subtracting the values of the UR image from that of the TR image might have been scattered because of possible differences between the ^{14}C intensities determined with UR-IP and those determined with TR-IP. To determine the noise levels due to this subtraction method, the ^{14}C-labeled graded standards (n = 10) were placed in contact with UR-IP for 2 wk and with TR-IP for another 2 wk. Circular ROIs (the area of each ROI was 0.0925 mm^2) were placed on the polymers of the ^{14}C-labeled graded standard of the UR image. We put the ROIs on the TR image at the same site as the UR image using the traced film. The noise level was defined as the s.d. of the difference between the ^{14}C intensities determined with UR-IP and those determined with TR-IP, which were corrected using the ^{14}C calibration lines (*15*).

TABLE 1
Noise Due to Subtraction Method

Polymer no.	^{14}C (UR)	^{14}C (TR corrected)	^{14}C (UR) − ^{14}C (TR corrected)	Noise level
1	446 ± 42	444 ± 40	2 ± 15	15
2	215 ± 22	214 ± 23	0 ± 11	11
3	107 ± 11	108 ± 11	−1 ± 7	7

^{14}C (UR) = ^{14}C intensity determined with UR-IP; ^{14}C (TR corrected) = ^{14}C intensity determined with TR-IP corrected using the ^{14}C calibration lines. The number of ROIs is 240 for each. Values are mean ± s.d. Unit is (PSL-BG)/mm^2 (PSL = unit of autoradiographic intensity; BG = background level) for each.

Statistical Analysis

The data are presented as mean ± s.d. The statistical significance of differences in mean values between Groups A and B was assessed with the two-tailed unpaired Student's t-test. The statistical significance of differences in mean values between the regions, between the ^{3}H- and the ^{14}C-labeled radiopharmaceutical uptake, was assessed with the two-tailed paired Student's t-test. The statistical significance of differences in mean values between rats with higher and lower ^{3}H-DG uptake in the normally perfused area was assessed with the Mann–Whitney U test. The two-factor analysis of variance with repeated measures on one factor was applied to compare the relationship between the percentage of blood flow and ^{3}H-DG uptake and between the percentage of blood flow and DG/BF between rats with higher and lower ^{3}H-DG uptake in the normally perfused area.

RESULTS

Noise Due to Subtraction Method

In Table 1, we show the noise level due to this subtraction method obtained with the ^{14}C-labeled graded standards. The noise level in the animal study was obtained with the standard polymer of ^{14}C, whose intensity was nearest to that in the region in each rat. In the border zone in Group A, ^{14}C and ^{3}H intensities were 111 ± 43 and 104 ± 60 (PSL-BG)/mm^2 (PSL, unit of autoradiographic intensity; BG, background level; n = 8), respectively. In this area, the noise level was 10 ± 6% of the ^{3}H intensity. In the peripheral ischemic area in Group B, ^{14}C and ^{3}H intensities were 74 ± 25 and 73 ± 14 (PSL-BG)/mm^2 (n = 8), respectively. In this area, the noise level was 10 ± 3% of the ^{3}H intensity.

Blood Flow versus Glucose Uptake

No significant difference in the plasma concentrations of glucose (12.7 ± 3.0 versus 11.1 ± 0.8 mmol/liter), insulin (6.5 ± 2.3 versus 9.5 ± 3.7 ng/ml) and free fatty acids (1.9 ± 1.1 versus 2.1 ± 0.9 mEq/liter) was found between Groups A and B. No significant difference in mean arterial pressure was found between Groups A and B before the LCA ligation (130 ± 14 versus 119 ± 17 mm Hg) or 30 min after the initiation of the LCA ligation (78 ± 31 versus 78 ± 16 mm Hg).

Figure 1 shows representative autoradiograms from the hearts of two rats in Group A. The border zone existed at the lateral borders (eight of eight rats), the subendocardial layer (eight of

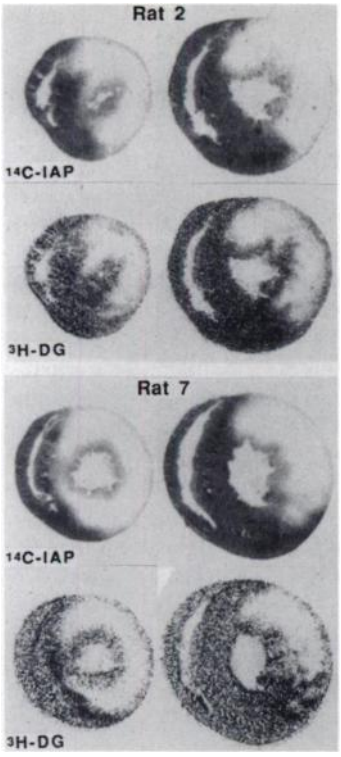

FIGURE 1. Double-tracer autoradiograms of apical (left panels) and midventricular (right panels) heart sections labeled with ^{14}C-IAP and ^{3}H-DG. At the lateral borders, subendocardial and the subepicardial layers are within the ischemic area, ^{3}H-DG uptake was preserved.

TABLE 2
Metabolic Characteristics

	^{3}H-DG uptake in Norm (Bq/mg)	Glucose (mmol/liter)	Insulin (ng/ml)	FFA (mEq/liter)
High-DG				
Rat 1	377	18.6	—	2.9
Rat 2	143	14.9	3.5	3.0
Rat 3	245	11.8	9.0	0.9
Rat 4	252	11.2	9.3	1.4
mean ± s.d.	254 ± 96*	14.1 ± 3.4	7.3 ± 3.3	2.1 ± 1.1
Low-DG				
Rat 5	70	14.0	7.8	3.1
Rat 6	71	11.8	4.2	2.6
Rat 7	55	9.5	5.7	1.2
Rat 8	29	9.8	6.0	0.2
mean ± s.d.	56 ± 20	11.3 ± 2.1	5.9 ± 1.5	1.8 ± 1.3

*$p < 0.05$ versus low-DG.

High- and low-DG are rats with higher and lower ^{3}H-DG uptake in the normally perfused area, respectively. Norm = normally perfused area; FFA = free fatty acids.

eight rats) and the subepicardial layer (four of eight rats) within the ischemic area (Fig. 2, left panels). Representative circumferential profile curves of the percentage of blood flow and the percentage of ^{3}H-DG uptake are shown in the right panels of Figure 2. The border zone occupied 36 ± 8% of the ischemic area (n = 8).

We divided all rats of Group A into two subgroups, high-DG (n = 4) and low-DG (n = 4). Tritium-DG uptake in the normally perfused area was significantly higher in high-DG than that in low-DG (Table 2). However, no significant difference was found in the plasma concentrations of glucose, insulin and free fatty acids between high- and low-DG. No significant difference was found between high- and low-DG in mean arterial pressure before (123 ± 13 versus 138 ± 10 mm Hg) or after (93 ± 37 versus 63 ± 18 mm Hg) the LCA ligation or in myocardial blood flow in the normally perfused area (79 ± 73 versus 114 ± 43 ml/100 g/min). In the border zone, ^{14}C and ^{3}H intensities were 93 ± 49 and 154 ± 40 (PSL-BG)/mm^2 in high-DG and 129 ± 33 and 54 ± 17 (PSL-BG)/mm^2 in low-DG, respectively. The noise level was 6 ± 2% and 14 ± 6% of the ^{3}H intensity in the border zone in high- and low-DG, respectively.

Tritium-DG uptake in the border zone was significantly lower than that in the normally perfused area in high-DG (Table

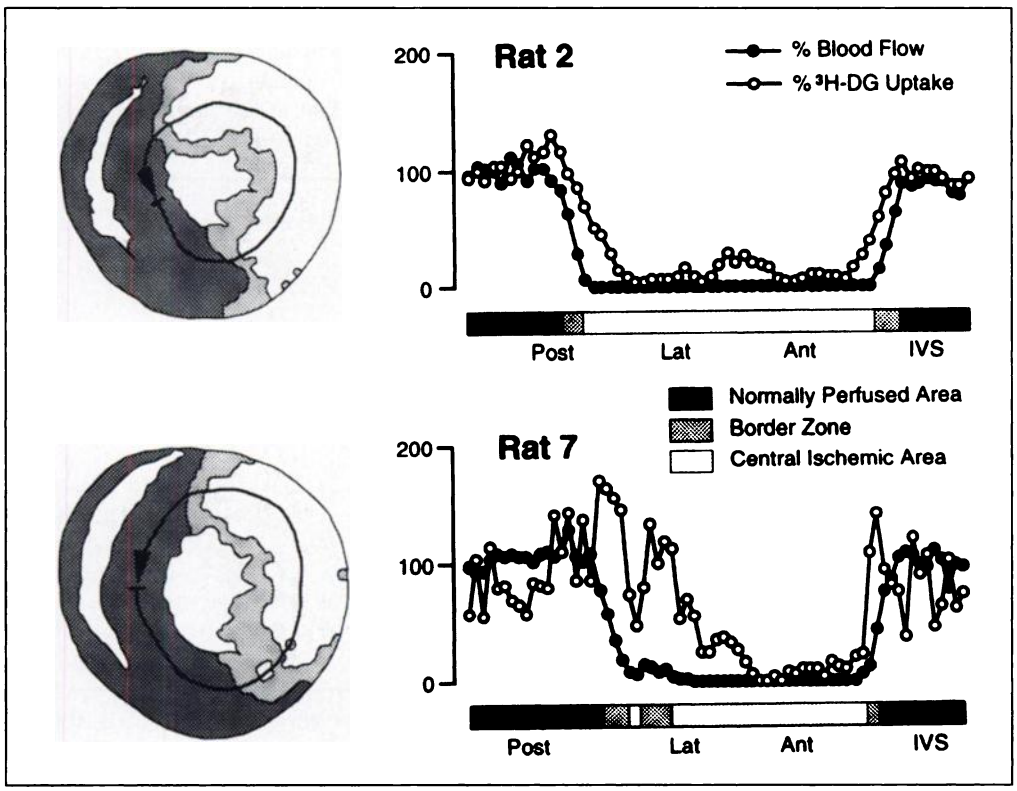

FIGURE 2. Spatial distributions of ischemic border zone reconstructed using quantitative data (left panels) and circumferential profile curves of percentage of blood flow and percentage of ^{3}H-DG uptake (right panels). Circumferential profile curves were obtained from values of ROIs placed in serial order in the midmyocardial layer of the left ventricular wall (arrows in left panels). IVS = interventricular septum; Post, Lat and Ant show the left ventricular posterior, lateral and anterior walls, respectively.

TABLE 3
Regional ^{3}H-DG Uptake and Blood Flow

	^{3}H-DG uptake (Bq/mg)	% ^{3}H-DG uptake	% Blood flow
High-DG			
Norm	254 ± 96*	100 ± 0	100 ± 0
Border zone	148 ± 52*†	59 ± 6*†‡	36 ± 2†
Central	33 ± 8*§	14 ± 6*‡	2 ±1§
Low-DG			
Norm	56 ± 20	100 ± 0	100 ± 0
Border zone	58 ± 15	108 ± 15‡	32 ± 3†
Central	20 ± 8§	36 ± 6‡§	3 ± 1§

*$p < 0.05$ versus low-DG.
†$P < 0.05$ versus Norm.
‡$p < 0.05$ versus percentage of blood flow.
§$p < 0.05$ versus Norm and border zone.
Norm = normally perfused area; central = central ischemic area.
High- and low-DG are rats with higher and lower ^{3}H-DG uptake in the normally perfused area, respectively. Values are mean ± s.d.

3). However, in low-DG, ^{3}H-DG uptake in the border zone was comparable with that in the normally perfused area. The percentage of ^{3}H-DG uptake in the border zone was significantly higher than the percentage of blood flow in both high- and low-DG.

In Figure 3, we show the relationship between the percentage of blood flow and absolute or relative ^{3}H-DG uptake in all rats of high- and low-DG. Absolute ^{3}H-DG uptake in the border zone was significantly higher in high-DG than in low-DG ($p < 0.05$ for each level of the percentage of blood flow) (Fig. 4). However, the percentage of ^{3}H-DG uptake in the border zone was significantly higher in low-DG than in high-DG ($p < 0.05$ for each level of the percentage of blood flow). A significant difference was found in the relationship between the percentage of blood flow and ^{3}H-DG uptake in the border zone between high- and low-DG ($p < 0.0005$). In high-DG, significant differences in ^{3}H-DG uptake were found among the regions in the border zone with 10%–19%, 20%–29%, 30%–39%, 40%–49%, 50%–59% and 60%–69% of the percentage of blood flow. That is, ^{3}H-DG uptake was lower in regions with smaller levels of the percentage of blood flow in high-DG. However, in low-DG, no significant differences in ^{3}H-DG uptake were found among the regions in the border zone with different levels of the percentage of blood flow except in the region with 10%–19% of the percentage of blood flow.

Absolute DG/BF in the normally perfused area and that in the border zone was significantly higher in high-DG than in low-DG (0.57 ± 0.51 versus 0.05 ± 0.01 and 1.06 ± 0.87 versus 0.21 ± 0.05 MBq · ml^{-1} · min, $p < 0.05$ for each). The percentage of DG/BF in the border zone was significantly lower in high-DG than in low-DG (192 ± 31% versus 408 ± 66%, $p < 0.05$). In high-DG, the absolute DG/BF in the border zone failed to reach a significant increase compared with that in the normally perfused area ($p = 0.07$). However, the percentage of DG/BF in the border zone was higher than that in the normally perfused area in high-DG ($p < 0.01$). In low-DG, both absolute DG/BF and the percentage of DG/BF in the border zone were higher than that in the normally perfused area ($p < 0.005$ for each). Figure 5 shows the relationship between the percentage of blood flow and absolute or relative DG/BF in the border zone. The increase in the percentage of DG/BF according to the decrease in the percentage of blood flow was steeper in low-DG than in high-DG ($p < 0.0005$).

These results did not differ when we analyzed the relationship between the percentage of blood flow and the rate of glucose uptake (*20*), determined using the time-activity curve of blood ^{3}H-DG and the plasma concentration of glucose.

Glucose Uptake Versus Fatty Acid Uptake

Figure 6 shows representative autoradiograms from the hearts of two rats in Group B. The peripheral ischemic area existed at the lateral borders (eight of eight rats), the subendocardial layer (five of eight rats) and the subepicardial layer (eight of eight rats) within the ischemic area. The peripheral ischemic area occupied 38% ± 15% of the ischemic area (n = 8). In the peripheral ischemic area, the percentage of ^{3}H-DG uptake was significantly higher than the percentage of ^{14}C-BMHDA uptake (Table 4).

The area ratio of the peripheral ischemic area of Group B was comparable with that of the border zone of Group A. No significant difference in ^{3}H-DG uptake in the normally perfused area was found between Groups A and B (155 ± 124 versus 105 ± 41 Bq/mg). Tritium-DG uptake in the border zone of Group A was comparable with that in the peripheral ischemic area of Group B (103 ± 60 versus 76 ± 12 Bq/mg).

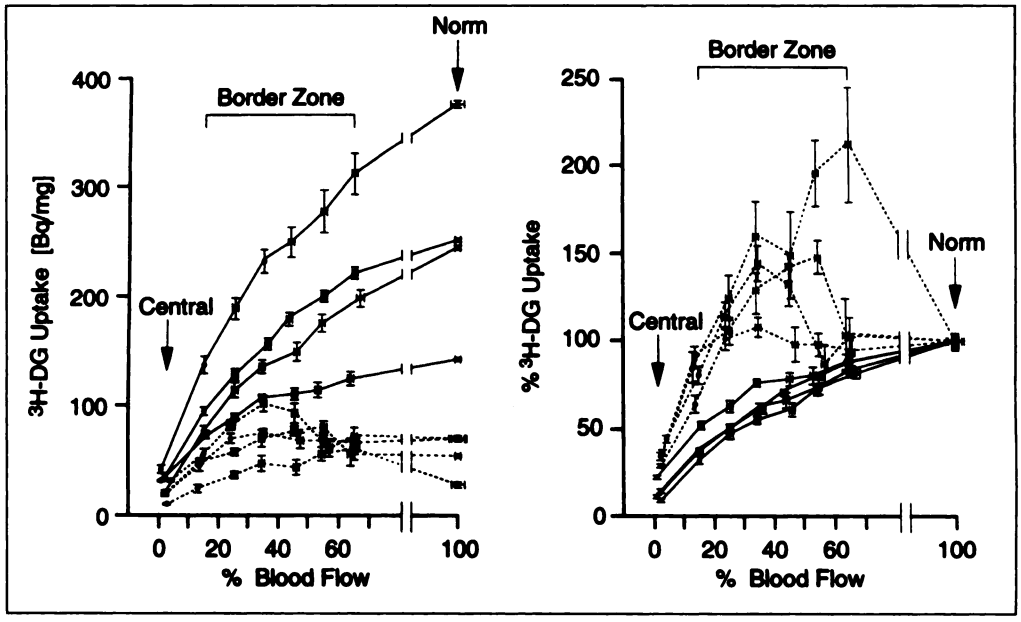

FIGURE 3. Relationship between percentage of blood flow and absolute or relative ^{3}H-DG uptake in all rats of high-DG (solid lines) and low-DG (broken lines). Each line was obtained from one rat. Values are mean ± s.e. of ROIs classified according to the percentage of blood flow. Norm = normally perfused area; central = central ischemic area.

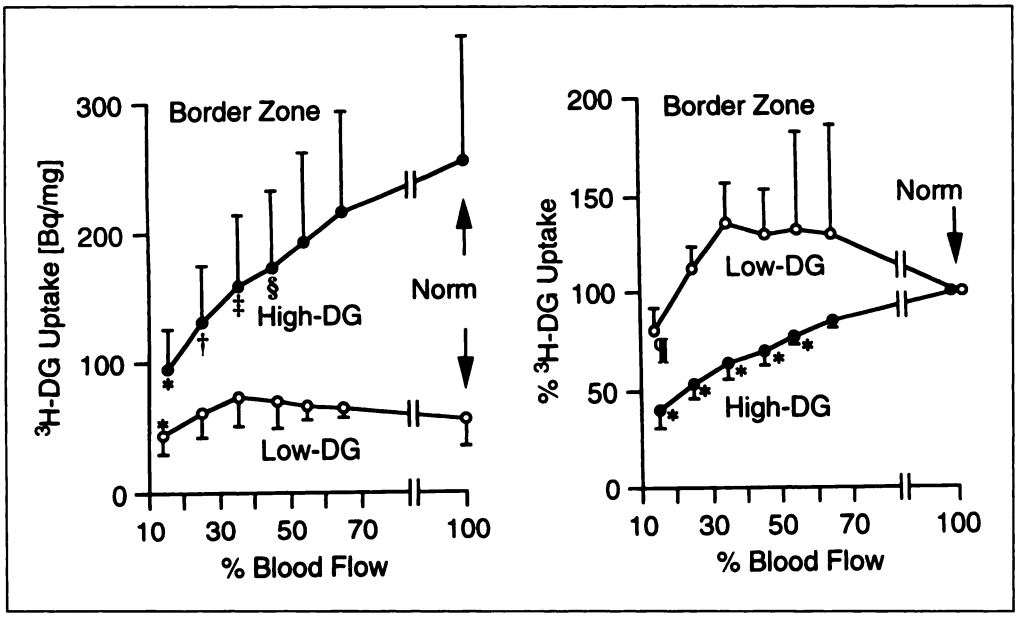

FIGURE 4. Relationship between percentage of blood flow and absolute or relative ^{3}H-DG uptake in the border zone in high- and low-DG (n = 4 for each). Values are mean ± s.d. Norm = normally perfused area. *p < 0.05 versus all other levels. †p < 0.05 versus 40%–49%, 50%–59% and 60%–69%. ‡p < 0.05 versus 50%–59% and 60%–69%. §p < 0.05 versus 60%–69%. ¶p < 0.05 versus 30%–39%, 40%–49%, 50%–59% and 60%–69% of the percentage of blood flow.

DISCUSSION

Glucose Uptake in the Ischemic Border Zone

This study clearly demonstrated that the relationship between blood flow and glucose uptake in the ischemic border zone is altered by the different glucose uptake levels in the normally perfused area. In rats with higher glucose uptake in the normally perfused area, glucose uptake in the border zone was reduced significantly according to the decrease in the percentage of blood flow. However, in rats with lower glucose uptake in the normally perfused area, no significant differences in glucose uptake were found among the regions in the border zone with different levels of the percentage of blood flow. In high-DG of this study, the glucose uptake reduced according to the decrease in the percentage of blood flow, which is assumed to reflect the reduced glucose supply. In low-DG, the percentage of DG/BF, which reflects the percentage of glucose extraction, increased steeply according to the decrease in the percentage of blood flow. Therefore, glucose uptake was preserved even in the regions with lower levels of glucose supply in low-DG.

Kalff et al. (*25*) showed, in dogs subjected to 40 min of coronary artery occlusion, that myocardial samples with more than 20% blood flow showed normal or near-normal ^{18}F-fluorodeoxyglucose (FDG) uptake, and the samples with more severe ischemia showed precipitously decreased FDG uptake with additional decrements in blood flow. Stanley et al. (*13*) decreased coronary arterial flow by 60% with an extracorporeal perfusion circuit and determined the glucose uptake and blood flow in swine hearts. They showed that regional glucose uptake in the ischemic area with 20% blood flow is not increased significantly compared with that in the normally perfused area (0.2–0.3 versus 0.2 μmol/g/min). More recently, Stanley et al. (*14*) demonstrated that regional glucose uptake in the ischemic area with 30%–40% blood flow is significantly higher than that in the normally perfused area (0.2–0.3 versus 0.04–0.05 μmol/g/min). These reports (*13,14*) are consistent with this study from the point of view that the relationship between glucose uptake in the ischemic area and that in the normally perfused area is altered by the different glucose uptake levels in the normally perfused area.

It also has been suggested that glucose uptake in the ischemic area may be fixed and may fail to respond to substrate availability and hormones (*13,14,25*). However, Mäki et al. (*26*) recently reported that glucose uptake can be increased strikingly by insulin in chronically dysfunctional but viable myocardium

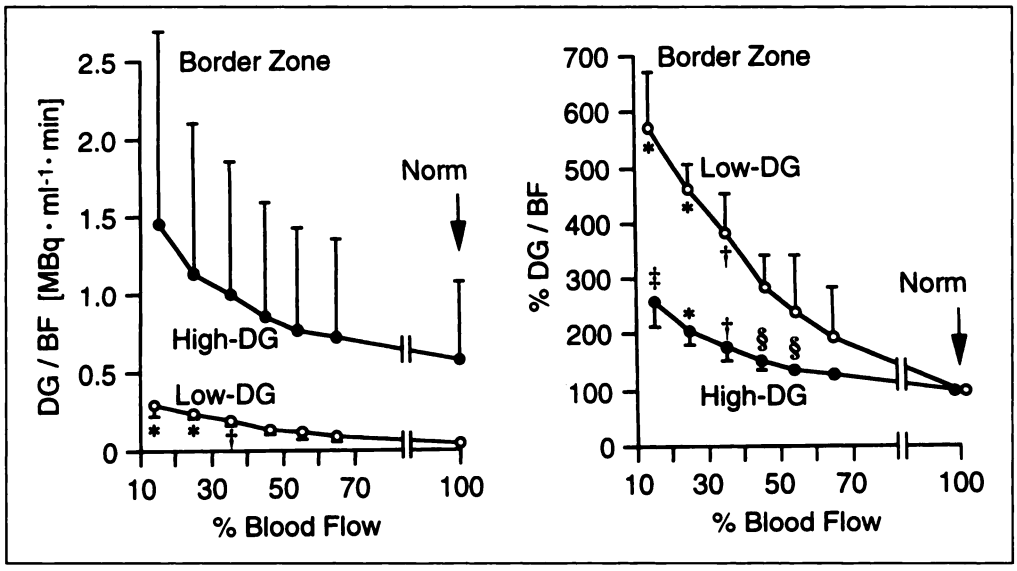

FIGURE 5. Relationship between the percentage of blood flow and absolute or relative ^{3}H-DG uptake per unit blood flow (DG/BF) in the border zone in high- and low-DG (n = 4 for each). Values are mean ± s.d. Norm = normally perfused area. *p < 0.05 versus 30%–39%, 40%–49%, 50%–59% and 60%–69%. †p < 0.05 versus 40%–49%, 50%–59% and 60%–69%. ‡p < 0.05 versus all other levels. §p < 0.05 versus 60%–69% of the percentage of blood flow.

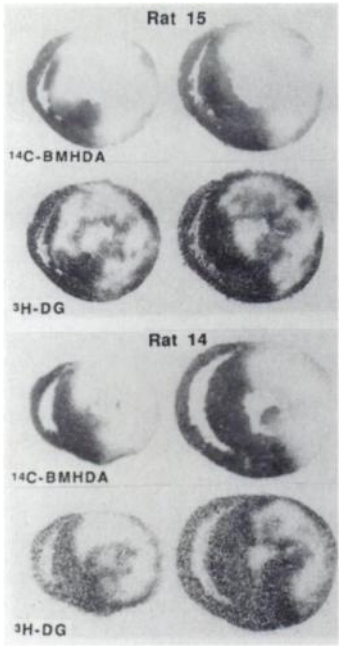

FIGURE 6. Double-tracer autoradiograms of apical (left panels) and midventricular (right panels) heart sections labeled with ^{14}C-BMHDA and ^{3}H-DG. Carbon-14-BMHDA uptake was greatly decreased in the ischemia area. However, ^{3}H-DG uptake was preserved at the lateral borders, the subendocardial and the subepicardial layers within the ischemic area.

in patients with coronary artery disease compared with that in the fasting state. This finding is consistent with this report suggesting that, in the border zone, glucose uptake stimulated by ischemia can be accelerated still more by humoral and mechanical factors.

Sun et al. (*27*) reported that translocation of the major myocardial glucose transporter, GLUT4, from an intracellular compartment to the plasma membrane, is induced by global ischemia. The combination of insulin plus ischemia stimulates to an even greater degree GLUT4 translocation compared with ischemia alone (*27*). In the ischemic border zone of this study, the GLUT4 translocation might be induced to a greater degree in high-DG than in low-DG.

Possible Limitations

In normally perfused myocardium, earlier studies from others showed that hyperinsulinemia and hyperglycemia increase glucose uptake, but high concentrations of free fatty acids decrease glucose uptake (*1,28*). Plasma concentrations of insulin, glucose and free fatty acids failed to reach significant differences between high- and low-DG in this study. This may be due to small numbers of rats of high- and low-DG. In addition, multiple factors including the plasma concentrations of insulin, glucose, free fatty acids and other humoral and mechanical factors might determine glucose uptake in the normally perfused area in this study.

TABLE 4
Regional ^{3}H-DG Uptake and ^{14}C-BMHDA Uptake

	^{3}H-DG uptake (Bq/mg)	% ^{3}H-DG uptake	% ^{14}C-BMHDA uptake
Norm	105 ± 41	100 ± 0	100 ± 0
Peripheral	76 ± 12	78 ± 18*†	27 ± 3*
Central	26 ± 6‡	27 ± 8†‡	3 ± 1‡

*$p < 0.05$ versus Norm.
†$p < 0.0005$ versus percentage of ^{14}C-BMHDA uptake.
‡$p < 0.05$ versus Norm and peripheral.
Values are mean ± s.d. n = 8 for each.
Norm = normally perfused area; peripheral = peripheral ischemic area; central = central ischemic area.

Hariharan et al. (*29*) showed that the relationship between myocardial uptake of glucose and deoxyglucose changed under non-steady-state conditions. Because myocardial glucose metabolism changes dynamically during acute ischemia (*30*), it would be difficult to determine absolute rates of glucose uptake in this study.

Clinical Implication

Glucose utilization in the ischemic area often has been analyzed by normalizing FDG uptake to that in the normally perfused area in patients with myocardial infarction (*4,5*). This study suggests that, in patients with high levels of glucose uptake in the normally perfused area, glucose uptake in the ischemic border zone may be estimated as "decreased" compared with that in the normally perfused area, even if the absolute value of glucose uptake is preserved. In PET studies, the underestimation of myocardial viability in the ischemic border zone might be caused by high plasma levels of insulin and glucose.

CONCLUSION

This study demonstrated that the relationship between blood flow and glucose uptake in the ischemic border zone was altered by the different glucose uptake levels in the normally perfused area. In addition, glucose uptake in the border zone was higher in rats with higher glucose uptake in the normally perfused area. This finding suggests that, in the border zone, glucose uptake stimulated by ischemia can be accelerated still more by humoral factors.

REFERENCES

1. Camici P, Ferrannini E, Opie LH. Myocardial metabolism in ischemic heart disease: basic principles and application to imaging by positron emission tomography. *Prog Cardiovasc Dis* 1989;32:217–238.
2. Rovetto MJ, Lamberton WF, Neely JR. Mechanisms of glycolytic inhibition in ischemic rat hearts. *Circ Res* 1975;37:742–751.
3. Opie LH. Effects of regional ischemia on metabolism of glucose and fatty acids: relative rates of aerobic and anaerobic energy production during myocardial infarction and comparison with effects of anoxia. *Circ Res* 1976;38:152–174.
4. Tillisch J, Brunken R, Marshall R, et al. Reversibility of cardiac wall-motion abnormalities predicted by positron tomography. *N Engl J Med* 1986;314:884–888.
5. Marwick TH, MacIntyre WJ, Lafont A, Nemec JJ, Salcedo EE. Metabolic responses of hibernating and infarcted myocardium to revascularization: a follow-up study of regional perfusion, function and metabolism. *Circulation* 1992;85:1347–1353.
6. Janse MJ, Cinca J, Moréna H, et al. The "border zone" in myocardial ischemia: an electrophysiological, metabolic and histochemical correlation in the pig heart. *Circ Res* 1979;44:576–588.
7. Hearse DJ, Yellon DM. The "border zone" in evolving myocardial infarction: controversy or confusion? *Am J Cardiol* 1981;47:1321–1334.
8. Buda AJ, Shlafer M, Gallagher KP. Spatial and temporal characteristics of circumferential flow-function relations during acute myocardial ischemia in the conscious dog. *Am Heart J* 1988;116:1514–1523.
9. David D, Michelson EL, Naito M, Dreifus LS. Extracellular potassium dynamics in the border zone during acute myocardial ischemia in a canine model. *J Am Coll Cardiol* 1988;11:422–430.
10. Hariman RJ, Louie EK, Krahmer RL, et al. Regional changes in blood flow, extracellular potassium and conduction during myocardial ischemia and reperfusion. *J Am Coll Cardiol* 1993;21:798–808.
11. Hoffman EJ, Huang SC, Phelps ME. Quantitation in positron emission computed tomography: 1. effect of object size. *J Comput Assisted Tomogr* 1979;3:299–308.
12. Takala TES, Hassinen IE. Effect of mechanical workload on the transmural distribution of glucose uptake in the isolated perfused rat heart, studied by regional deoxyglucose trapping. *Circ Res* 1981;49:62–69.
13. Stanley WC, Hall JL, Stone CK, Hacker TA. Acute myocardial ischemia causes a transmural gradient in glucose extraction but not glucose uptake. *Am J Physiol* 1992;262:H91–H96.
14. Stanley WC, Hall JL, Smith KR, Cartee GD, Hacker TA, Wisneski JA. Myocardial glucose transporters and glycolytic metabolism during ischemia in hyperglycemic diabetic swine. *Metabolism* 1994;43:61–69.
15. Yamane Y, Ishide N, Kagaya Y, et al. Quantitative double-tracer autoradiography with tritium and carbon-14 using imaging plates: application to myocardial metabolic studies in rats. *J Nucl Med* 1995;36:518–524.
16. Slein MW, Cori GT, Cori CF. A comparative study of hexokinase from yeast and animal tissues. *J Biol Chem* 1950;186:763–780.
17. Hengartner H, Zuber H. Isolation and characterization of a thermophilic glucokinase from Bacillus stearothermophilus. *FEBS Lett* 1973;37:212–216.
18. Yalow RS, Berson SA. Immunoassay of endogenous plasma insulin in man. *J Clin Invest* 1960;39:1157–1175.

19. Shimizu S, Inoue K, Tani Y, Yamada H. Enzymatic microdetermination of serum-free fatty acids. *Anal Biochem* 1979;98:341–345.
20. Sokoloff L, Reivich M, Kennedy C, et al. The [^{14}C]deoxyglucose method for the measurement of local cerebral glucose utilization: theory, procedure and normal values in the conscious and anesthetized albino rat. *J Neurochem* 1977;28:897–916.
21. Sakurada O, Kennedy C, Jehle J, Brown JD, Carbin GL, Sokoloff L. Measurement of local cerebral blood flow with iodo[^{14}C]antipyrine. *Am J Physiol* 1978;234:H59–H66.
22. Livni E, Elmaleh DR, Levy S, Brownell GL, Strauss HW. Beta-methyl[1-^{11}C]heptadecanoic acid: a new myocardial metabolic tracer for positron emission tomography. *J Nucl Med* 1982;23:169–175.
23. Abendschein DR, Fox KAA, Ambos HD, Sobel BE, Bergmann SR. Metabolism of beta-methyl[1-^{11}C]heptadecanoic acid in canine myocardium. *Nucl Med Biol* 1987; 14:579–585.
24. Hoffman EJ, Phelps ME, Weiss ES, et al. Transaxial tomographic imaging of canine myocardium with ^{11}C-palmitic acid. *J Nucl Med* 1977;18:57–61.
25. Kalff V, Schwaiger M, Nguyen N, McClanahan TB, Gallagher KP. The relationship between myocardial blood flow and glucose uptake in ischemic canine myocardium determined with fluorine-18-deoxyglucose. *J Nucl Med* 1992;33:1346–1353.
26. Mäki M, Luotolahti M, Nuutila P, et al. Glucose uptake in the chronically dysfunctional but viable myocardium. *Circulation* 1996;93:1658–1666.
27. Sun D, Nguyen N, DeGrado TR, Schwaiger M, Brosius FC III. Ischemia induces translocation of the insulin-responsive glucose transporter GLUT4 to the plasma membrane of cardiac myocytes. *Circulation* 1994;89:793–798.
28. Saddik M, Lopaschuk GD. Myocardial triglyceride turnover and contribution to energy substrate utilization in isolated working rat hearts. *J Biol Chem* 1991;266:8162–8170.
29. Hariharan R, Bray M, Ganim R, Doenst T, Goodwin GW, Taegtmeyer H. Fundamental limitations of [^{18}F]2-deoxy-2-fluoro-D-glucose for assessing myocardial glucose uptake. *Circulation* 1995;91:2435–2444.
30. Neely JR, Whitmer JT, Rovetto MJ. Effect of coronary blood flow on glycolytic flux and intracellular pH in isolated rat hearts. *Circ Res* 1975;37:733–741.

Comparison of Modified Technetium-99m Albumin and Technetium-99m Red Blood Cells for Equilibrium Ventriculography

Anne-Sophie E. Hambÿe, Kristin A. Verbeke, Rudi P. Vandermeiren, Eric J. Joosens, Alfons M. Verbruggen and Michel J. De Roo

Nuclear Medicine and Radiotherapy Departments, Middelheim General Hospital, Antwerp; and Radiopharmacy and Nuclear Medicine Departments, University of Leuven, Leuvin, Belgium

A newly developed modified form of ^{99m}Tc-labeled human serum albumin reconstituted from a kit (^{99m}Tc-dimercaptopropionyl-human serum albumin; ^{99m}Tc-DMP-HSA) was prospectively compared to ^{99m}Tc-labeled red blood cells (RBC) in patients referred for equilibrium radionuclide ventriculography at rest to evaluate its potential use as a blood-pool imaging agent. **Methods:** A Paired comparison between ^{99m}Tc-DMP-HSA and either in vitro or in vivo ^{99m}Tc-labeled RBC was performed within 2 days in 20 patients. For each study, two sets of images were acquired, starting at 15 min and 180 min postinjection, respectively. Each set consisted of a gated blood-pool cardiac study and a planar static image centered on the patient's thorax. All data were processed by two independent observers. Early and late postinjection parameters were calculated: ejection fraction (EF) value, activity within the main organs surrounding the left ventricle (LV), ratio of activity between the LV and these surrounding organs for each study separately, and temporal (late/early) evolution of the intraorgan activities and of the LV/organ ratios after decay correction. **Results:** The images and the visual wall-motion analysis were of good quality with both agents in most patients, without significant image degradation at 180 min postinjection. Calculated EF values were highly comparable with the two tracers. Interobserver variability was 0.17% (RBC) and 1.08% (DMP-HSA) for the early EF value (EF1), and 0.62% (RBC) and 0.27% (DMP-HSA) for the late EF (EF2). Mean difference between EF2 and EF1 was 0.74% (Observer 1) and 0.28% (Observer 2) for ^{99m}Tc-RBC, and −2.88% (Observer 1) and −2.07% (Observer 2) for ^{99m}Tc-DMP-HSA. When comparing ^{99m}Tc-DMP-HSA to ^{99m}Tc-RBC the mean difference was 1.27% (Observer 1) and 0.36% (Observer 2) for EF1, and −2.35% (Observer 1) and −1.99% (Observer 2) for EF2. Also, the biodistribution and temporal evolution of the organ repartition of both compounds were stable and similar, with values of late/early activity ratios very close to one for all the studied organs [mean intraorgan ratio: 0.946 for ^{99m}Tc-RBC (range: 0.881–1.086) and 0.979 for ^{99m}Tc-DMP-HSA (range: 0.914–1.141); mean late/early LV/organ ratio: 0.964 for ^{99m}Tc-RBC (range: 0.919–1.016) and 0.967 for ^{99m}Tc-DMP-HSA (range: 0.912–1.035)]. **Conclusion:** Paired comparison of kit-prepared ^{99m}Tc-DMP-HSA to ^{99m}Tc-labeled RBC demonstrated that both agents were very closely related regarding as well the calculated EF value as the in vivo stability up to more than 3 hr postinjection. Technetium-99m-DMP-HSA may constitute a practical and useful replacement for ^{99m}Tc-labeled RBC.

Key Words: technetium-99m-DMP-HSA; technetium-99m-labeled red blood cells; gated blood-pool imaging

J Nucl Med 1997; 38:1521–1528

During the past two decades, radionuclide ventriculography has been one of the main performed tests in nuclear cardiology, earning a well-established position in cardiology because of its reliability and reproducibility in the assessment of left ventricular function, which is the most frequently used parameter in the evaluation of cardiac performance (*1–10*). Nevertheless, the future of this technique could be threatened by the rapid growth of alternative imaging modalities such as echocardiography (*11*), ultrafast computed tomography (*12*) and nuclear MRI (*13*). Since all these methods suffer from some restrictions such as observer experience (*14,15*), high cost or limited availability, radionuclide angiography still enjoys an important position in the field of noninvasive functional imaging modalities. However, further developments are certainly required to ensure its maintenance as one of the references of left ventricular function assessment.

Two ^{99m}Tc-labeled agents, autologous radiolabeled red blood cells (^{99m}Tc-RBC) and human serum albumin (^{99m}Tc-HSA) are at our disposal to measure the ejection fraction (EF) in daily practice. Due to the relatively weak binding of the radionuclide to the protein and the resulting important and rapid extravascular diffusion, radiolabeled albumin is not the agent of first choice (*16,17*). Therefore, in vitro or in vivo labeled RBC are the preferred radiopharmaceutical in many nuclear medicine departments (*18*), despite the practical disadvantages of time and labor consumption and the necessary manipulation of blood samples with potential risk of contamination (*19–21*). More-

Received Jun. 4, 1996; revision accepted Nov. 14, 1996.

For correspondence or reprints contact: A.-S. Hambÿe, Department of Nuclear Medicine, Middelheim General Hospital, Lindendreef 1, 2020 Antwerp, Belgium.